JACS
JOURNAL OF THE AMERICAN CHEMICAL SOCIETY

Communication

pubs.acs.org/JACS

Coordination-Based Molecular Assemblies as Electrochromic Materials: Ultra-High Switching Stability and Coloration Efficiencies

Sreejith Shankar, Michal Lahav, and Milko E. van der Boom*

Department of Organic Chemistry, Weizmann Institute of Science, Rehovot 7610001, Israel

Web-Enhanced Feature Supporting Information

ABSTRACT: We demonstrate high-performance electrochromic assemblies that exhibit a practical combination of low-voltage operation and efficient electrochromic switching as well as long-term thermal and redox stability (1.12×10^5 cycles). Our molecular assemblies can be integrated into a solid-state configuration. Furthermore, we also show how the molecular structure of the chromophores correlates with the materials' growth and function. The coloration efficiencies of our assemblies are higher than those of inorganic materials and many conducting polymers, in addition to offering an alternative fabrication approach.

Polymer-based devices find widespread applications in display technology, solar cells, electro-optic modulators, and sensors. The large display technology market and the demand for smart windows are driving the development of electrochromic (EC) polymers.[1−4] Applicable EC materials should exhibit a combination of properties that includes the following: (i) long-term redox and photochemical stability, (ii) high contrast ratios, (iii) high coloration efficiencies, (iv) controllable switching times, and (v) color homogeneity. Processability is also a key parameter. Reynolds has demonstrated color tuning of EC materials by varying the substitutions on EC polymers.[5] Conjugated polymers have characteristically low band gaps, and high oxidation states can be achieved.[6,7] In contrast to the well-developed polymer chemistry,[8] relatively few examples of molecular assemblies with EC properties are known.[9] Moreover, their integration into solid-state devices is rare.[10] The above-mentioned requirements limit the pool of suitable chromophores. Among the candidates, metal polypyridyl and related complexes are considered ideal chromophores for fabricating EC materials because of their excellent stability and light absorption that significantly depends on their oxidation state.[11−16] In addition, color tunability can be achieved through structural control and molecular design.

In this study we used a dip-coating process to generate molecular assemblies (**MA1−4**) with exceptional coloration efficiencies and redox stability. Moreover, we demonstrate how a first generation solid-state setup is formed. **MA1−4** were obtained by alternating the deposition of $PdCl_2$ and iron polypyridyl complexes **1−4** (Figure 1) from solution on a pyridine-terminated monolayer.[17] This monolayer is covalently bound to the surfaces of indium−tin oxide (ITO), quartz, and silicon substrates through a chlorobenzyl-functionalized coupling layer (Scheme S1, Figure S2). Pyridine-based ligands are excellent moieties for η^1-coordination with d^8 palladium salts[18] and involve *trans*-(N_{Py}-N_{Py}) with a four-coordinate square planar geometry. Other first-row transition-metal salts could also be used.[19,20] Pd(II)-ligand coordination has been utilized to generate well-defined structures in solution and solid-state materials.[17,21,22]

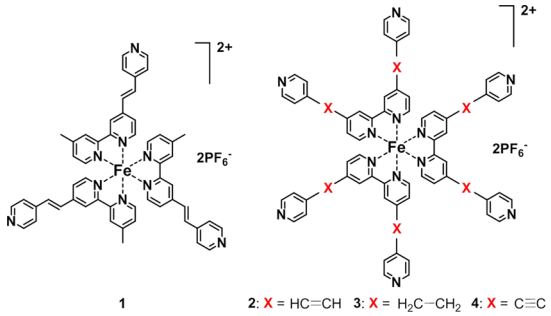

Figure 1. Molecular structures of polypyridyl complexes **1−4**.

The MAs have been characterized by optical (UV−vis, ellipsometry, Raman) spectroscopy, X-ray photoelectron spectroscopy (XPS), electrochemistry, and spectroelectrochemistry (SEC). Our data indicate that the film growth (linear or expontential) is affected by the number of pyridine binding sites. **MA1** exhibits exponential growth versus the number of deposition cycles (Figure 2A), similarly to previously reported osmium polypyridyl complexes.[9] We have shown that these self-propagating MAs store an excess of $PdCl_2$ that can be used to induce the here observed exponential growth. In contrast to **MA1**, **MA2−4** exhibit linear growth behavior (Figures 2B, S3), because the sterically more demanding complexes **2−4** allow less Pd to be stored in the assemblies (Figure S2). Indeed, XPS analysis revealed that the excess of Pd content is 73% higher for **MA1** and only 25% higher for **MA2** than what one would expect for the formation of a fully formed network. Raman intensity ($\nu_{C=C}$ = 1610 cm^{-1}) as a function of the number of deposition cycles also corroborates the exponential or linear growth behavior of **MA1** and **MA2**, respectively (Figures 2D, S4). The linear correlation between the ellipsometry-derived thickness and absorbance maxima confirms the uniformity of all the MAs and the substrate independent growth behavior (SiO_x vs quartz).

Interestingly, varying the number of pyridine moieties and the pyridine-bipyridine bond order (H_2C−CH_2, HC=CH,

Received: January 16, 2015
Published: March 2, 2015

DOI: 10.1021/jacs.5b00429
J. Am. Chem. Soc. 2015, 137, 4050−4053

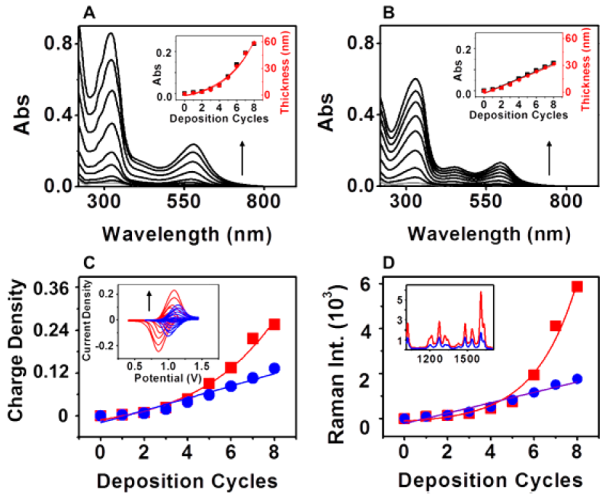

Figure 2. Growth behavior of **MA1** and **MA2**. Optical absorption spectra of (A) **MA1** and (B) **MA2** after each deposition cycle of complex **1** or **2**, respectively, and $PdCl_2$. Insets: Intensities of absorption bands at λ = 575 nm (**MA1**) and λ = 591 nm (**MA2**) (left axis, black) and the ellipsometry-derived thickness (right axis, red). (C) Total ejected charge: **MA1** (red) and **MA2** (blue). The charge density is shown in mC/cm^2. Inset: Corresponding CVs of **MA1** (red) and **MA2** (blue). The current density is shown in mA/cm^2. (D) Raman intensity (ν = 1610 cm^{-1}). Inset: Raman spectra of **MA1** (red) and **MA2** (blue) (8 deposition cycles) (R^2 > 0.93 for all fits). For magnified versions of the insets, see Figures S6, S8.

C≡C) have been used this study to obtain different colors, to control the electrochemical properties, and the redox stability of the assemblies while using the same dip-coating process. The four MAs have the following colors: **MA1**: purple, **MA2**: bluish gray, **MA3**: pinkish, and **MA4**: gray (Figures 3 insets; S5). The MAs exhibit metal-to-ligand charge transfer (MLCT) bands at λ = 535−591 nm (Figures 2A,B, S3). **MA2**−**4** exhibit another defined MLCT band at a lower wavelength (370−450 nm); the

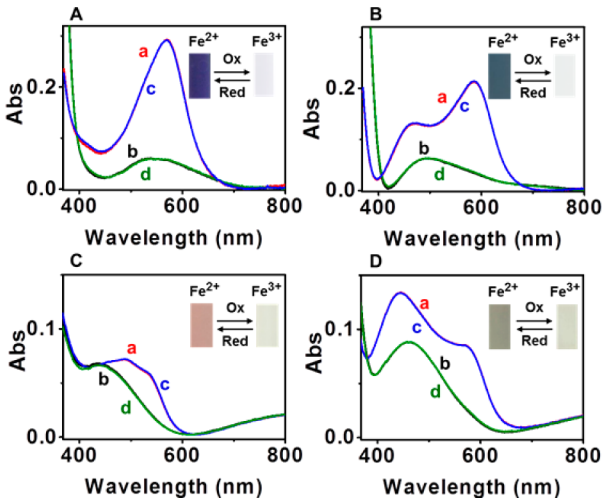

Figure 3. EC switching of the MAs. Optical absorption spectra corresponding to the consecutive oxidation and reduction of (A) **MA1**, (B) **MA2**, (C) **MA3**, and (D) **MA4**. The switching was done using double-potential steps between 0.4 and 1.7 V (**MA1**, **MA2**), 0.2 and 1.6 V (**MA3**), and 0.5 and 1.9 V (**MA4**). (a, c) reduced (Fe^{2+}), (b, d) oxidized (Fe^{3+}) states. Inset: photographs of **MA1**−**4** showing the colored (Fe^{2+}) and the bleached (Fe^{3+}) states.

combination of these two bands gives rise to the observed colors. Similar MLCT bands have been reported for other polypyridine-based Fe(II) complexes.[23,24]

The electrochemical and spectroelectrochemical properties of the MAs have been evaluated after 8 deposition cycles. For instance, cyclic voltammetry (CV) measurements of **MA1** and **MA2** on ITO revealed reversible redox processes characteristic of a $Fe^{2+/3+}$ couple with half-wave potentials ($E_{1/2}$) of 0.96 and 1.08 V, respectively (vs Ag/Ag^+; a scan rate of 100 mVs^{-1}) (Figures 2C inset, S6). The peak current density and total charge (obtained by integrating the voltammetric peaks) increase exponentially with increasing deposition cycles for **MA1** and linearly for **MA2** (Figures 2C, S7). These observations are in agreement with the above-mentioned optical data and indicate that the growth of these assemblies is independent of the nature of the substrate (SiO_x vs ITO).

For both MAs, the peak current density is linearly proportional to the scan rate (0.100−0.700 V/s) (Figure S9), indicative of a surface-confined electrochemical oxidation−reduction process that is not limited by slow diffusion.[25] A linear correlation between the absorption maxima (MLCT) and the current density indicates that all metal centers are electroactive up to 8 deposition cycles (Figure S10, Table S1). Electrochemical profiles similar to **MA2** were obtained for **MA3** and **MA4** (Figure S11).

The single electron oxidation−reduction processes are accompanied by a reversible change in the coloration of the MAs. Upon oxidation ($Fe^{2+} \rightarrow Fe^{3+}$), the intensities of the MLCT bands are significantly reduced, resulting in the disappearance of color, as observable by the naked eye (Figure 3; Video 1 and Video 2).

The UV−vis data show that complexes **1** and **2** (X = HC═CH) form assemblies that have higher contrast ratios than do the assemblies formed with complexes **3** or **4** (X = H_2C−CH_2 or X = C≡C) (Figure 1). Therefore, the SEC properties of **MA1** and **MA2** were studied by applying double potential steps as a function of time (chronoamperometry). The optical response was recorded at λ = 575 nm (**MA1**) and λ = 591 nm for (**MA2**) as the percentage of transmittance (%T) over time. These MAs have high contrast ratios [$\Delta\%T_{max}$ = 41 (**MA1**), 31 (**MA2**)] that can be changed as a function of the pulse width (0.25−10 s) and the viscosity of the solvent (acetonitrile, 0.37 mPa·s; propylene carbonate, 2.5 mPa·s, at 25 °C). The lower viscosity of acetonitrile allows faster ionic diffusion of the supporting electrolyte.[26] A near maximum $\Delta\%T$ (>98%) was observed for both MAs with a pulse width of 1−2 s in ACN (Figure 4). The response time was found to be thickness dependent. For instance, **MA1** has a response time of ∼0.40 s after 5 deposition cycles, which doubles to ∼0.80 s after 8 deposition cycles. No evidence for any redox events related to Pd(II) in these assemblies was observed in the potential window −1 V to +2 V. The combination of low-voltage operation (∼1.0 V) and a fast response time of ∼0.30 s (>95% oxidation and reduction) for **MA2** makes it an excellent EC assembly (Figure S12).

The low charge needed to switch between the redox states results in exceptionally high values of coloration efficiency (CE): **MA1** = 955 cm^2 C^{-1} (λ = 575 nm) and **MA2** = 1488 cm^2 C^{-1} (λ = 591 nm). The CE of **MA1** is higher (>2×) in comparison with the assemblies constructed from *iso*-structural osmium complexes having a similar stability.[9] This key parameter reflects the performance and power efficiency of EC materials and is defined as the change in optical density

DOI: 10.1021/jacs.5b00429
J. Am. Chem. Soc. 2015, 137, 4050−4053

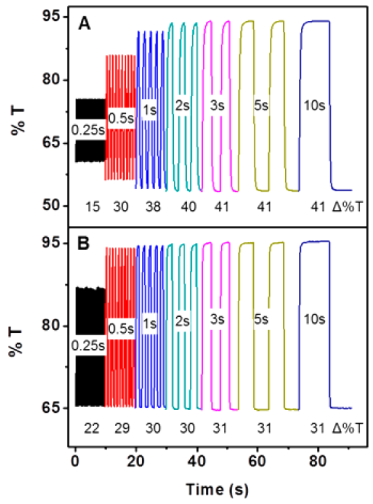

Figure 4. Chronoabsorptometry of **MA1** and **MA2** at different switching times. These experiments (λ = 575 nm, **MA1**; λ = 591 nm, **MA2**) were carried out at room temperature in 0.1 M $TBAPF_6$/ACN using ITO-coated glass as the working electrode, Pt wire as the counter electrode, and Ag/Ag^+ as the reference electrode.

(ΔOD) per unit charge injected/ejected per unit area of the electrode.

The exceptional stability of the **MA2** was demonstrated by electrochemistry, SEC experiments, and thermal exposure. This assembly is electrochemically stable up to 1.12×10^5 redox cycles (Figure 5A,B). Optical changes were recorded for 3.0×10^4 times at λ = 591 nm with a pulse width of 1 s without appreciable performance loss (Figure 5C). The SEC stability of the other MAs was determined by measuring the contrast ratio for 1000 redox cycles. Whereas **MA2** is highly stable, loss of contrast ratio was observed for **MA1** (−10%), **MA3** (−39%), and **MA4** (−28%). The stability of **MA2** might be attributed to the judicious combination of two key factors: electron density on the terminal pyridines and conjugation of the ligand framework. The electron density on the pyridine groups affects the coordination to Pd(II), whereas the conjugation might allow extended delocalization of electrons and/or positive charges.[27] **MA1**−**2** are stable at 70 °C for at least up to 150 days in air, as shown by UV−vis spectroscopy (Figures 5D,E, S13).

The feasibility of MA-based devices was demonstrated by covering our nanoscale thick films with a gel-electrolyte and a top ITO electrode (Figure 6). EC switching between the colored and transmissive states was observed with this solid-state setup using potential steps of −2.7 to 2.5 V (**MA1**) and −3 to +3 V (**MA2**) with a pulse width of 5 s.

In conclusion, the stimuli-responsive materials introduced here can be fine-tuned to be thermally robust and have exceptionally high (spectro)electrochemical stabilities. The large number of redox cycles demonstrated here are two orders of magnitude higher than known structurally related molecular assemblies.[9] Many polymeric EC materials,[28] including systems that contain polypyridyl complexes exhibit lower EC stabilities. Varying the number of pyridine moieties of the chromophores can be used to control (i) the materials' stability, (ii) color, (iii) redox chemistry, and (iv) their film growth (i.e., linear vs exponential). Our observations also demonstrate that minor structural differences (i.e., the pyridine-bipyridine bond order) at the molecular level become apparent

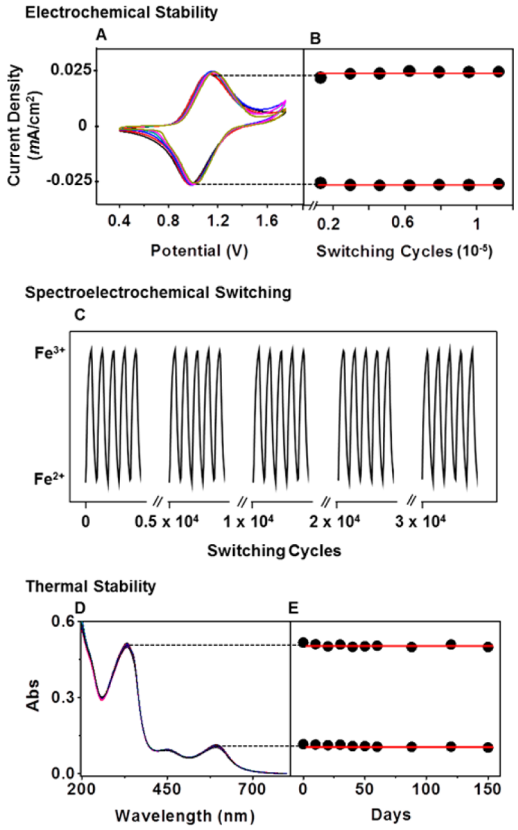

Figure 5. Stability of **MA2**. (A) CV of **MA2** up to 1.12×10^5 switching cycles. (B) Maximum current as in (A) vs the number of switching cycles. (C) SEC of **MA2** on ITO at 591 nm over a potential range of 0.55−1.45 V with a 1 s pulse width. Each segment in (C) corresponds to the first five switching cycles of every interval. The CV and the SEC measurements were carried out using a 0.1 M Bu_4NPF_6/PC electrolyte solution. (D) UV−vis spectra of **MA2** (on a quartz substrate) kept at 70 °C for 150 days. (E) The absorbance maxima as in (D) of the π−π^* band (332 nm) and the MLCT band (591 nm).

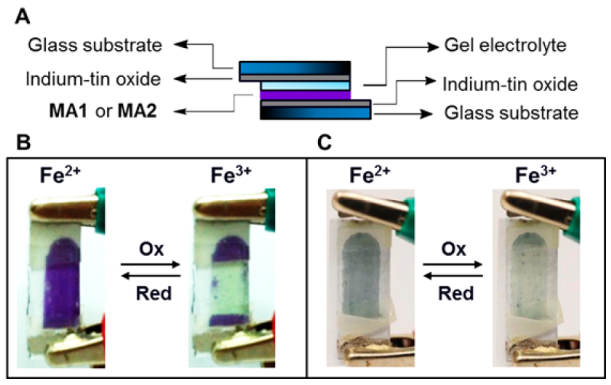

Figure 6. MA-based solid-state setup. (A) Device cross-section. (B, C) photographs showing the device's operation. Potential windows of −2.7 to +2.5 V (**MA1**) and −3 to +3 V (**MA2**) were applied with a pulse width of 5 s. The gel electrolyte (ACN:PC:PMMA:$(CF_3SO_2)_2N$-Li^+ 70:20:7:3 wt % composition) was drop casted and cured at 60 °C for 10 min.

in stability and EC performance. Another important property of our materials is the extremely high CEs. These efficiencies surpass the CEs of inorganic materials and most conducting polymers.[28] EC coatings are mainly prepared by spin coating and electropolymerization.[3,4,29] Our alternative layer-by-layer

DOI: 10.1021/jacs.5b00429
J. Am. Chem. Soc. 2015, 137, 4050−4053

approach is also suitable for the preparation of highly effective EC films. Metallopolymers based on bipyridine complexes were extensively studied electrochemically by Murray and others.[30−33] To this end, we have shown for the first time that coordination-based molecular assemblies are potentially useful materials for generating EC devices.[10,34,35]

■ ASSOCIATED CONTENT

Ⓢ Supporting Information

Experimental methods and more characterization data. This material is available free of charge via the Internet at http://pubs.acs.org.

Ⓦ Web-Enhanced Features

Two videos showing coloration of the MAs.

■ AUTHOR INFORMATION

Corresponding Author

*milko.vanderboom@weizmann.ac.il

Notes

The authors declare no competing financial interest.

■ ACKNOWLEDGMENTS

This research was supported by the Helen and Martin Kimmel Center for Molecular Design, The Schmidt Minerva Center, the Nofar program, and the Alternative Sustainable Energy Research Initiative (AERI). M.E.vdB. is the incumbent of the Bruce A. Pearlman Professorial Chair in Synthetic Organic Chemistry.

■ REFERENCES

(1) Thakur, V. K.; Ding, G.; Ma, J.; Lee, P. S.; Lu, X. *Adv. Mater.* **2012**, *24*, 4071.
(2) Gunbas, G.; Toppare, L. *Chem. Commun.* **2012**, *48*, 1083.
(3) Beaujuge, P. M.; Reynolds, J. R. *Chem. Rev.* **2010**, *110*, 268.
(4) Mortimer, R. J. *Annu. Rev. Mater. Res.* **2011**, *41*, 241.
(5) Amb, C. M.; Dyer, A. L.; Reynolds, J. R. *Chem. Mater.* **2010**, *23*, 397.
(6) Kobayashi, M.; Colaneri, N.; Boysel, M.; Wudl, F.; Heeger, A. J. *J. Chem. Phys.* **1985**, *82*, 5717.
(7) Kumar, A.; Bokria, J. G.; Buyukmumcu, Z.; Dey, T.; Sotzing, G. A. *Macromolecules* **2008**, *41*, 7098.
(8) Beaujuge, P. M.; Ellinger, S.; Reynolds, J. R. *Nat. Mater.* **2008**, *7*, 795.
(9) Motiei, L.; Lahav, M.; Freeman, D.; van der Boom, M. E. *J. Am. Chem. Soc.* **2009**, *131*, 3468.
(10) Yasuda, T.; Tanabe, K.; Tsuji, T.; Coti, K. K.; Aprahamian, I.; Stoddart, J. F.; Kato, T. *Chem. Commun.* **2010**, *46*, 1224.
(11) Puodziukynaite, E.; Oberst, J. L.; Dyer, A. L.; Reynolds, J. R. *J. Am. Chem. Soc.* **2011**, *134*, 968.
(12) Sortino, S.; Petralia, S.; Conoci, S.; Di Bella, S. *J. Am. Chem. Soc.* **2003**, *125*, 1122.
(13) Guo, Z.; Shen, Y.; Wang, M.; Zhao, F.; Dong, S. *Anal. Chem.* **2003**, *76*, 184.
(14) Rubinstein, I.; Bard, A. J. *J. Am. Chem. Soc.* **1980**, *102*, 6641.
(15) Nie, H.-J.; Zhong, Y.-W. *Inorg. Chem.* **2014**, *53*, 11316.
(16) Han, F. S.; Higuchi, M.; Kurth, D. G. *J. Am. Chem. Soc.* **2008**, *130*, 2073.
(17) Kaminker, R.; Motiei, L.; Gulino, A.; Fragalà, I.; Shimon, L. J. W.; Evmenenko, G.; Dutta, P.; Iron, M. A.; van der Boom, M. E. *J. Am. Chem. Soc.* **2010**, *132*, 14554.
(18) Chakrabarty, R.; Mukherjee, P. S.; Stang, P. J. *Chem. Rev.* **2011**, *111*, 6810.
(19) Richter, S.; Traulsen, C. H. H.; Heinrich, T.; Poppenberg, J.; Leppich, C.; Holzweber, M.; Unger, W. E. S.; Schalley, C. A. *J. Phys. Chem. C* **2013**, *117*, 18980.
(20) Gupta, T.; Mondal, P. C.; Kumar, A.; Jeyachandran, Y. L.; Zharnikov, M. *Adv. Funct. Mater.* **2013**, *23*, 4227.
(21) Stone, M. T.; Moore, J. S. *J. Am. Chem. Soc.* **2005**, *127*, 5928.
(22) Drain, C. M.; Lehn, J.-M. *Chem. Commun.* **1994**, 2313.
(23) Coe, B. J.; Fielden, J.; Foxon, S. P.; Brunschwig, B. S.; Asselberghs, I.; Clays, K.; Samoc, A.; Samoc, M. *J. Am. Chem. Soc.* **2010**, *132*, 3496.
(24) Machan, C. W.; Adelhardt, M.; Sarjeant, A. A.; Stern, C. L.; Sutter, J.; Meyer, K.; Mirkin, C. A. *J. Am. Chem. Soc.* **2012**, *134*, 16921.
(25) Shiryaeva, I. M.; Collman, J. P.; Boulatov, R.; Sunderland, C. J. *Anal. Chem.* **2003**, *75*, 494.
(26) Chiang, T.-Y.; Huang, M.-C.; Tsai, C.-H. *RSC Adv.* **2014**, *4*, 21201.
(27) Damrauer, N. H.; Boussie, T. R.; Devenney, M.; McCusker, J. K. *J. Am. Chem. Soc.* **1997**, *119*, 8253.
(28) Sonmez, G.; Meng, H.; Wüdl, F. *Chem. Mater.* **2004**, *16*, 574.
(29) Sassi, M.; Salamone, M. M.; Ruffo, R.; Mari, C. M.; Pagani, G. A.; Beverina, L. *Adv. Mater.* **2012**, *24*, 2004.
(30) Abruna, H. D.; Denisevich, P.; Umana, M.; Meyer, T. J.; Murray, R. W. *J. Am. Chem. Soc.* **1981**, *103*, 1.
(31) Zhu, S. S.; Swager, T. M. *J. Am. Chem. Soc.* **1997**, *119*, 12568.
(32) Forster, R. J.; Walsh, D. A.; Mano, N.; Mao, F.; Heller, A. *Langmuir* **2004**, *20*, 862.
(33) For an example of electrochemical studies of metal-organic films, see: Sakamoto, R.; Katagiri, S.; Maeda, H.; Nishimori, Y.; Miyashita, S.; Nishihara, H. J. *J. Am. Chem. Soc.* **2015**, *137*, 734.
(34) Wang, J.; Zhang, L.; Yu, L.; Jiao, Z.; Xie, H.; Lou, X. W.; Wei Sun, X. *Nat. Commun.* **2014**, *5*, 4921.
(35) Dyer, A. L.; Bulloch, R. H.; Zhou, Y.; Kippelen, B.; Reynolds, J. R.; Zhang, F. *Adv. Mater.* **2014**, *26*, 4895.

DOI: 10.1021/jacs.5b00429
J. Am. Chem. Soc. 2015, 137, 4050−4053